Supplemental Methods

Animals. Male C57Bl/6 mice (n=27) were obtained from Charles River (Sulzfeld, Germany) and housed in groups of 5-10 in individually ventilated BCU cages within a temperature controlled facility on a 14h/10h light/dark cycle. To obtain a range of glucose uptake values, mice were divided into four groups: i) no intervention (n=10); ii) extended fasting (18h) in home cage, to lower ^{18}F-FDG uptake (n=5); iii) pretreatment with insulin (6 mU/kg) and glucose (1 g/kg) ip 30 min prior to ^{18}F-FDG, to stimulate myocardial glucose uptake (n=5), under standard isoflurane anesthesia (1.5-2%, 0.6 L/min O_2) during image acquisition; or iv) ketamine (84 mg/kg, ip) and xylazine (11.8 mg/kg, ip) anesthesia, to suppress myocardial glucose uptake (n=7). Excluding fasting protocols, mice had free access to standard laboratory diet (Altromin, Lage, Germany) and drinking water.

PET Imaging. Dynamic acquisitions were performed using a dedicated small animal PET camera (Inveon DPET, Siemens). Anesthetized mice were positioned prone in the imaging chamber with the head placed in the anesthetic nose cone. The imaging chamber was then positioned to place the heart at the centre field of view. The tail veins were dilated using warm water, and a cannula was inserted into a lateral tail vein. ^{18}F-FDG (7.7±0.9 MBq) was injected in a 0.1-0.15 mL bolus of isotonic saline over 20s. The cannula line was then flushed with 0.1 mL of saline. Dynamic listmode data were acquired over 60 min. Electrocardiograms and respiration were monitored continuously using BioVet software, and isoflurane was adjusted to maintain a regular respiratory frequency (60-80 min^{-1}). Ketamine-xylazine anesthesia was effective for ~90min after injection. Blood glucose concentration was measured from a peripheral vein just prior to ^{18}F-FDG injection and at the conclusion of the PET scan using a glucose meter (Contour XT, Bayer Vital, Leverkusen, Germany).

Image Reconstruction. Listmode data of 60 min scans were histogrammed to 32 frames (5×2s, 4×5s, 3×10s, 8×30s, 5×60s, 4×300s, and 3×600s). Images were reconstructed to a 128x128x159 image matrix (0.78x0.78x0.80mm) using an ordered subset expectation maximization 3-dimensional / maximum a posteriori (OSEM3D/fastMAP) algorithm (β = 1, OSEM subsets = 16, OSEM iterations = 2, MAP iterations = 18, constant resolution prior) with scanner-applied scatter correction and a target resolution of 1.2 mm. An external source transmission scan was obtained for each mouse and used for attenuation correction (paired 185 MBq ^{57}Co sources, 10 min acquisition).

Image Analysis and Kinetic Modeling. Image analysis was completed using PMOD 3.6 software (PMOD Technologies, Zurich, Switzerland). A 3D volume of interest was defined for the left ventricle using interactive thresholding and adjusted manually to define appropriate myocardial contours (vol = 111±36 mm^3). Early frames (0-10s) were used to manually define distinct VOIs for the blood pool: a) 4.2 mm^3 sphere (r=1mm) placed in the centre of the left ventricle cavity, b) 4.2 mm^3 sphere placed on the left atrial cavity, or c) 12.6 mm^3 cylinder (r=1mm) placed on the inferior vena cava, rostral to renal branches and caudal to the diaphragm (Fig S1). The vena cava VOI covered a wider area than in comparable reports (*1*), which used only a single slice. Transaxial radii were kept constant to minimize the difference in partial volume losses between the blood pool VOIs.

Myocardium time activity curves were fitted to a Patlak kinetic model (*2*) using the PKIN module (PMOD Technologies, Zurich, Switzerland), using each of the blood pool time-activity curves as IDIF. A number of fit criteria were applied to the kinetic data to compare the Patlak fit over the full course of the 60 min acquisition. The applied parameters included: a) automated fit without exclusion; b) fit from 10 min (late fit) excluding the early rapid uptake component of the

time-activity curve; or c) fit from 0-10 min (early fit) excluding the plateau component of the time-activity curve. The automated fit considers all 32 points of the curve at equal weighting, generating a linear line of best fit from the earliest aligned timepoint. A limit of 20% variance from the linear line of best fit was applied, such that points outside this range were excluded from the analysis. Rate of myocardial glucose uptake (rMGU) was calculated as $rMGU = K_i \times (BG/LC)$; where K_i is the graphically-defined Patlak slope, BG is the average blood glucose concentration of start and end of the scan, and LC is the lumped constant = 0.67 estimated for rodents (*3*).

For validation, the integral of each IDIF volume was calculated over the first 2 min, first 5 min, first 10 min, and complete acquisition. Dynamic myocardial ^{18}F-FDG uptake was calculated from the average voxel intensity (Bq/cc) in the myocardial VOI and the injected dose (Bq) to yield a percent injected dose per gram (%ID/g). Uptake values were calculated at early (10-20min), intermediate (20-30min) and late (50-60min) timepoints to obtain a semi-quantitative indication of ^{18}F-FDG kinetics.

Statistics. All data are presented as mean values ± standard deviation. Statistical comparisons were completed using SPSS 18.0 software. Group data were analysed using one-way analysis of variance with Tukey's *post hoc* corrections for multiple comparisons. Pearson product-moment correlation coefficients were calculated between Patlak slopes obtained with different IDIF volumes or fit limits. Kinetic data was further contrasted using Bland Altman analysis. Population variability (σ) was calculated as the standard deviation divided by the mean. $P<0.05$ was considered to be significant.

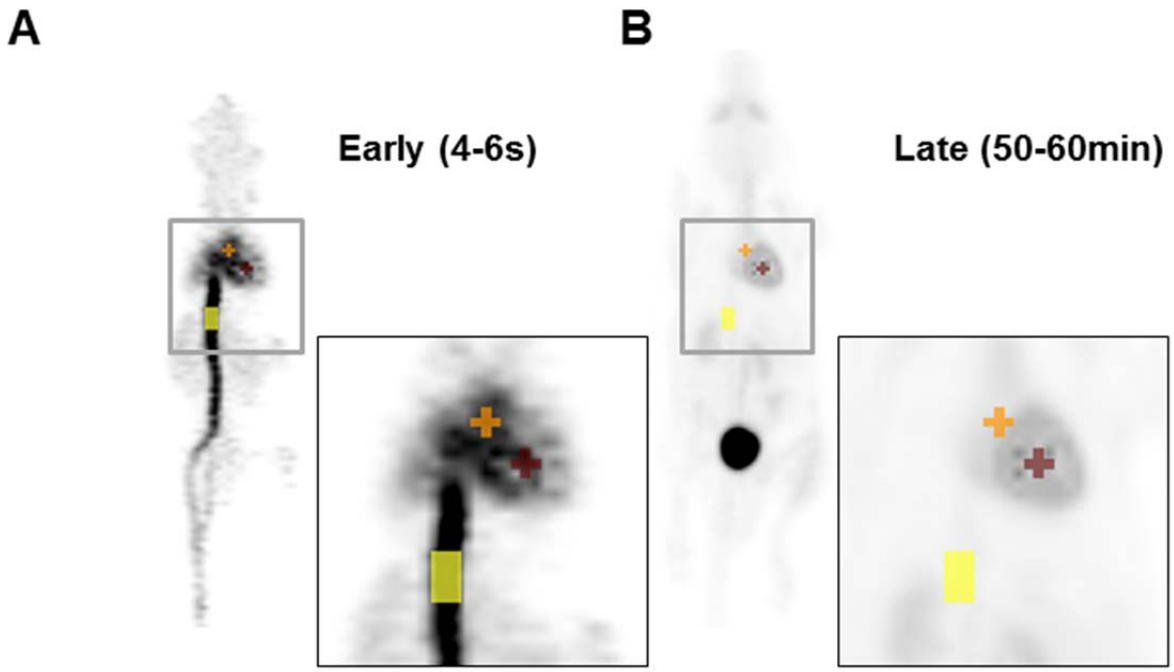

Supplemental Fig. 1. Sample volumes of interest used to define the input function. (**A**) Early frame (4-6s) and (**B**) late frame (50-60 min) 3D maximum intensity projection ^{18}F-FDG image in a control mouse. Regions of interest for left ventricle cavity (red), left atrial cavity (orange), and inferior vena cava rostral to the renal branches (yellow) are illustrated.

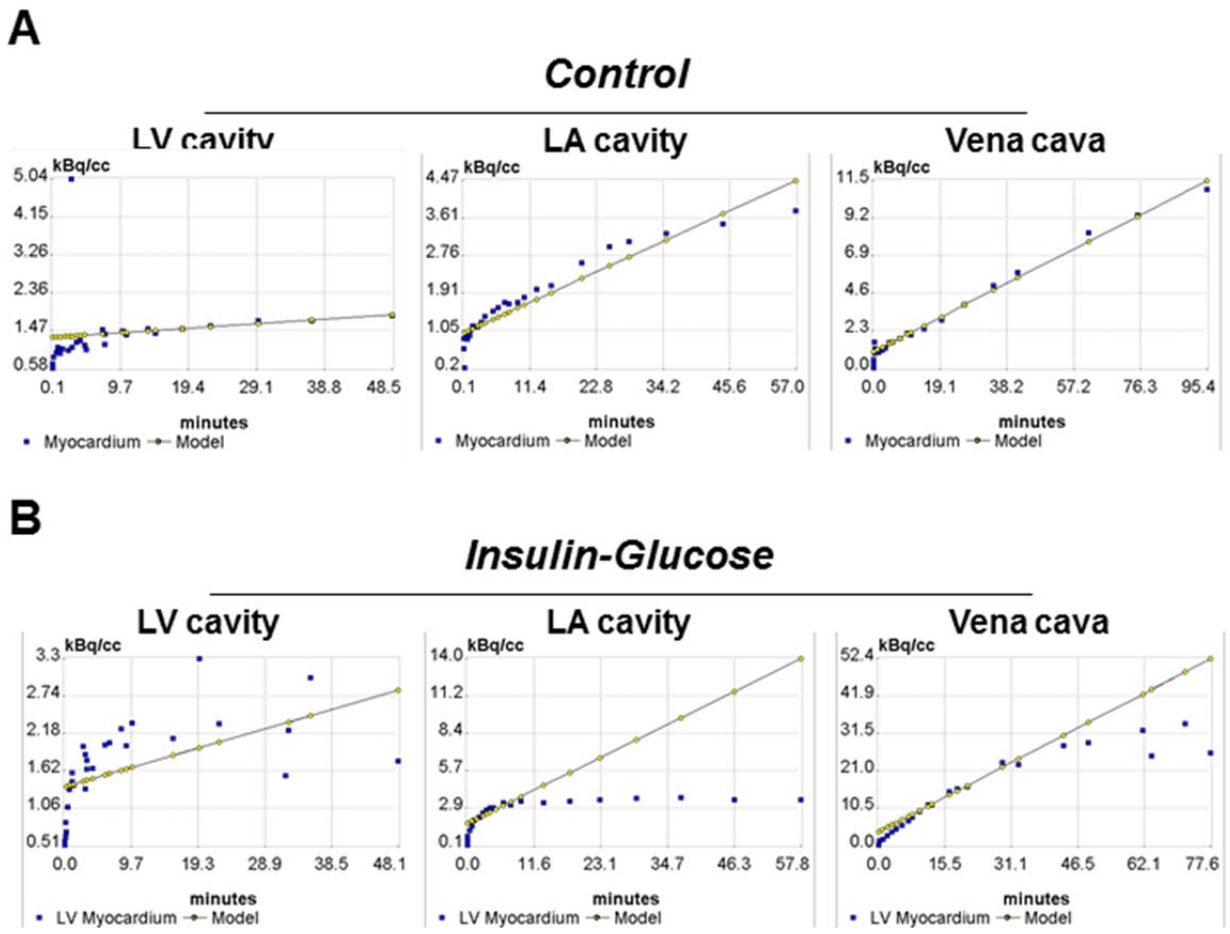

Supplemental Fig. 2. Representative Patlak graphs for each experimental group. Patlak plots for left ventricle myocardium prepared using the inferior vena cava as the input function are displayed for control, insulin-glucose, extended fasting, ketamine-xylazine. Note the dramatic differences in the y axis scales.

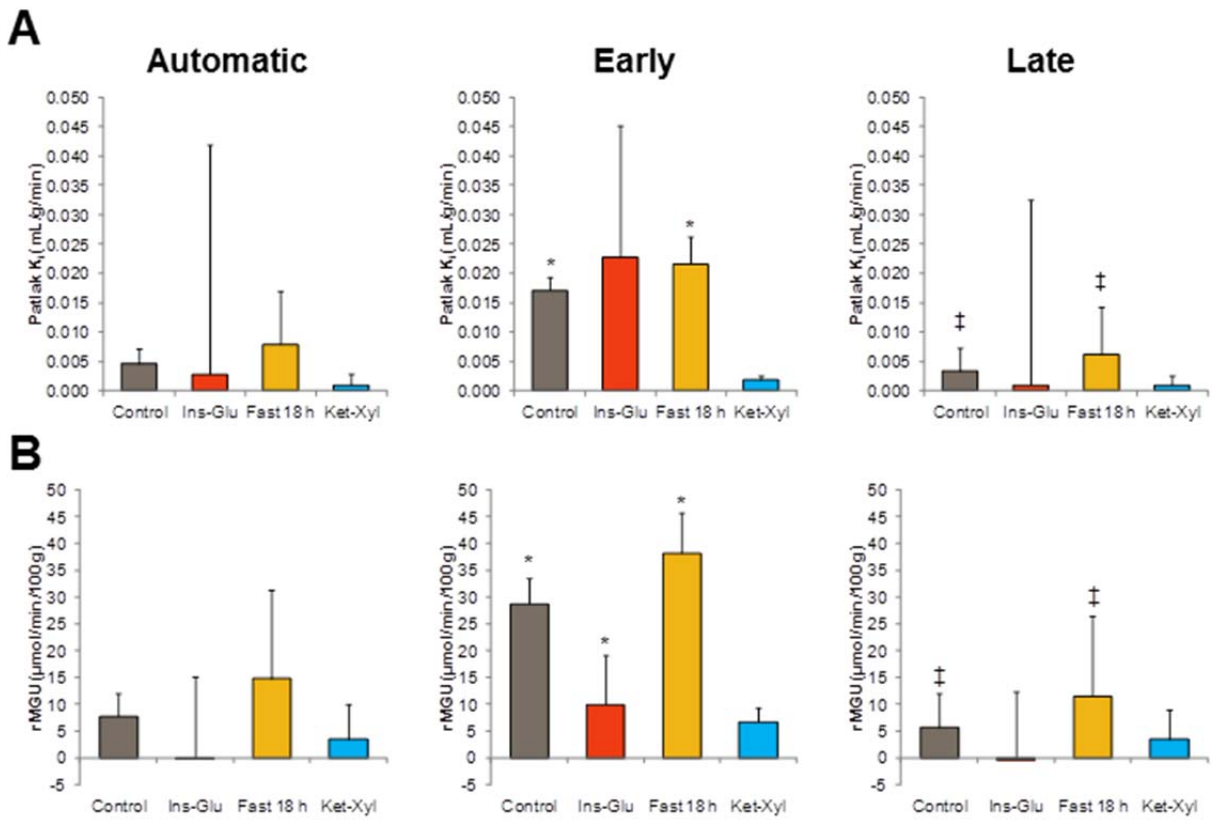

Supplemental Fig. 3. Impact of modified temporal limits for kinetic fit on Patlak calculations. (**A**) Patlak slope (K_i) value and (**B**) rate of myocardial glucose uptake (rMGU) when applying automated fit to the full myocardial time activity curve (automatic), restricting the fit from 2-40min (early), or restricting the fit to 10-60min (late) using the left ventricle cavity blood pool as the input function. Population variability for each group is increased and the Patlak estimates markedly reduced as compared to inferior vena cava or left atrial cavity image-derived input function, reflecting the elevated blood pool activity in late frames due to spillover from the myocardium. * $p<0.05$ to automatic fit, ‡ $p<0.05$ to early fit, matched group, Student's paired t-test.

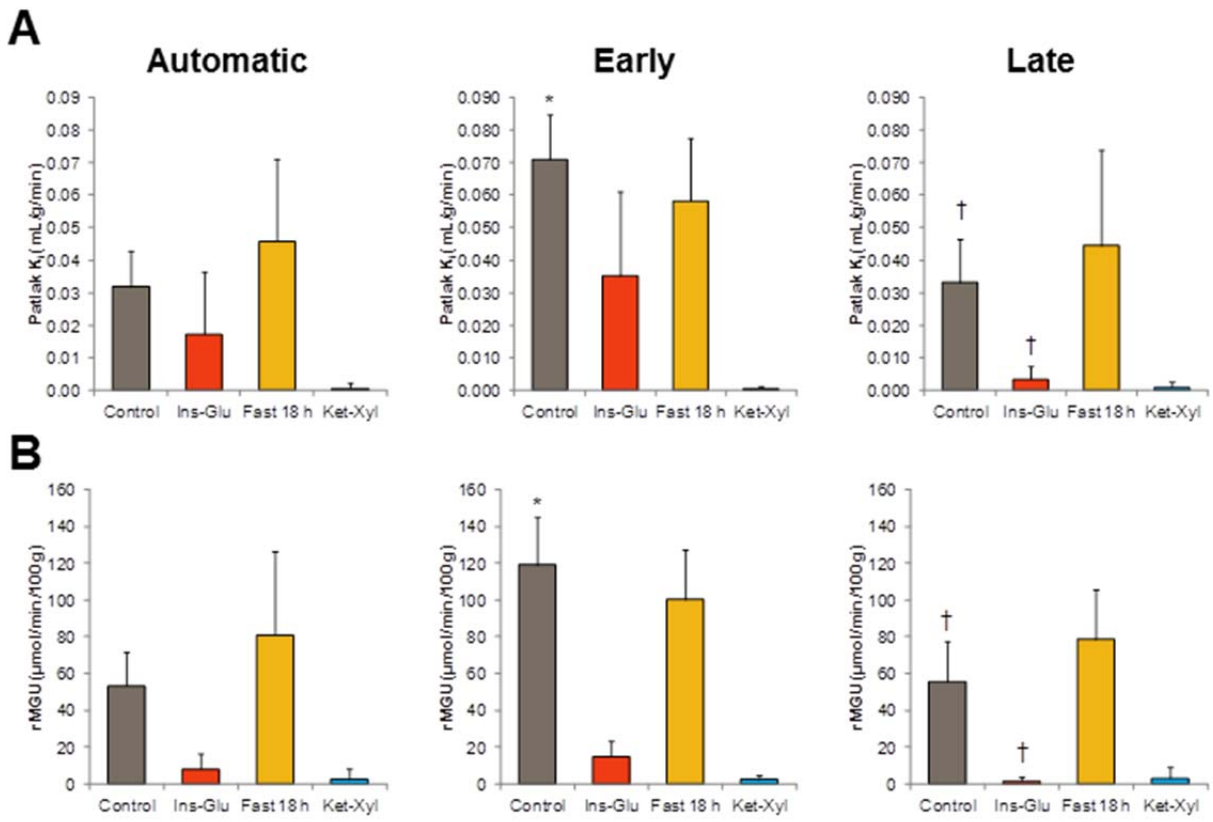

Supplemental Fig. 4. Impact of modified temporal limits for kinetic fit on Patlak calculations. (**A**) Patlak slope (K_i) value and (**B**) rate of myocardial glucose uptake (rMGU) when applying automated fit to the full myocardial time activity curve (automatic), restricting the fit from 2-40min (early), or restricting the fit to 10-60min (late) using the left atrial cavity blood pool as the input function. Patlak values are markedly lower as compared to the inferior vena cava image-derived input function, reflecting the elevated blood pool activity in late frames due to spillover from the myocardium. * $p<0.05$ to automatic fit, ‡ $p<0.05$ to early fit, matched group, Student's paired t-test.

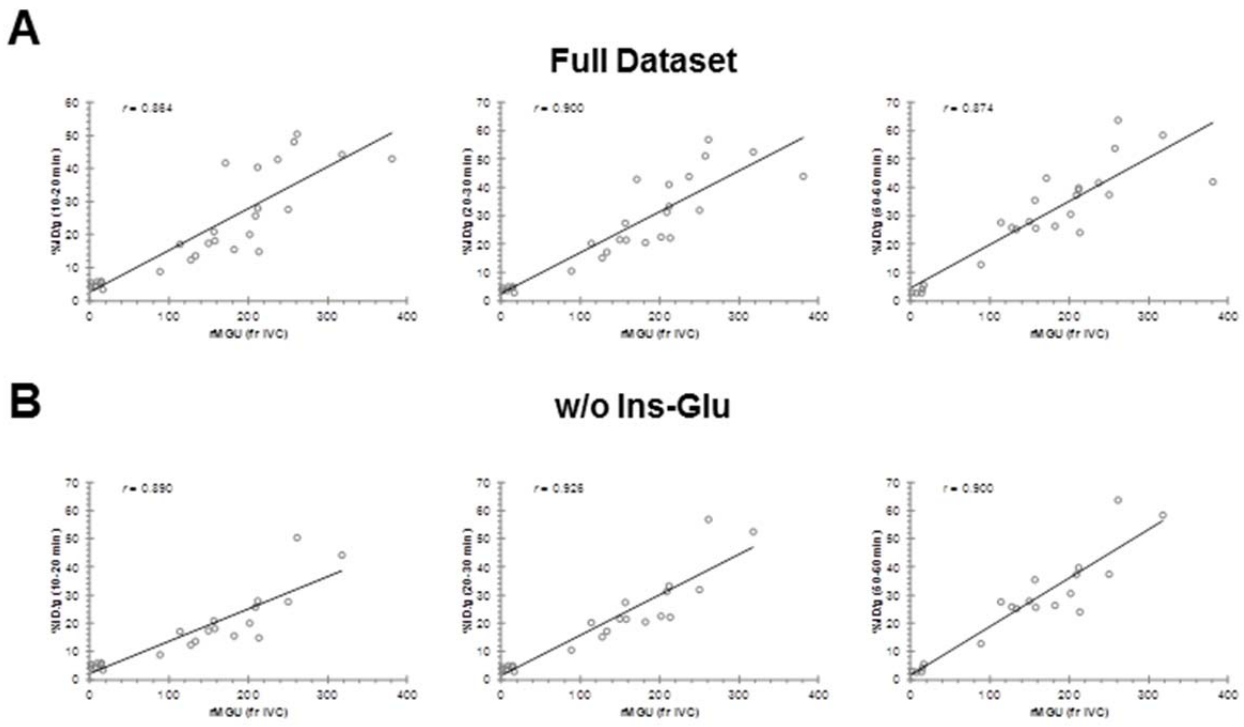

Supplemental Fig. 5. Pearson correlation of Patlak values with semi-quantitative ^{18}F-FDG uptake. Correlation of rate of myocardial glucose uptake (rMGU) to serial %ID/g (**A**) including and (**B**) excluding insulin-glucose group. Correlation tends to be stronger than Patlak slope.

References

1. Croteau E, Renaud JM, Archer C, et al. beta2-adrenergic stress evaluation of coronary endothelial-dependent vasodilator function in mice using C-acetate micro-PET imaging of myocardial blood flow and oxidative metabolism. *EJNMMI Res.* 2014;4:68.

2. Phelps ME, Huang SC, Hoffman EJ, Selin C, Sokoloff L, Kuhl DE. Tomographic measurement of local cerebral glucose metabolic rate in humans with (F-18)2-fluoro-2-deoxy-D-glucose: validation of method. *Ann Neurol.* 1979;6:371-388.

3. Thorn SL, deKemp RA, Dumouchel T, et al. Repeatable noninvasive measurement of mouse myocardial glucose uptake with 18F-FDG: evaluation of tracer kinetics in a type 1 diabetes model. *J Nucl Med.* 2013;54:1637-1644.